ELSEVIER

Journal of Physics and Chemistry of Solids 61 (2000) 1855–1864

JOURNAL OF PHYSICS AND CHEMISTRY OF SOLIDS

www.elsevier.nl/locate/jpcs

Deep levels including lattice relaxation: first- and second-neighbor effects

Charles W. Myles[a,*], Wei-Gang Li[b]

[a]*Department of Physics and Engineering Physics, Texas Tech University, Box 41051, Lubbock, TX 79409-1051, USA*
[b]*Alcatel Corporation, Plano, TX 75075, USA*

Received 8 December 1999; accepted 27 March 2000

Abstract

The effects of lattice relaxation on the deep levels due to substitutional impurities in semiconductors are investigated using an extension of a previously developed formalism. Both first- and second-neighbor relaxation are included in the formalism. Using this method, deep level chemical trends and their trends with varying amounts of lattice relaxation are explored. For specific impurities, molecular dynamics is used to calculate the lattice relaxation around an impurity, and its effects on the deep levels are computed using a Green's function technique. The results of the application of this theory to several impurities in Si, GaAs, and GaP are presented and compared with experiment and other theories.

PACS: 71.55. − i; 71.55.Eq; 71.55.Cn

Keywords: A. Semiconductors; D. Defects; D. Electronic structure

1. Introduction

The properties of a semiconductor are strongly influenced by defects which produce deep levels in the bandgap [1–9]. Unlike shallow levels [10], which are produced by the long-ranged Coulomb potential of a defect and which primarily control the magnitude and type of the conductivity, deep levels are produced by the central-cell, atomic-like defect potential and primarily control the charge-carrier lifetime [1–9]. Shallow levels are well described by effective mass theory [10]. Starting about two decades ago, many theories, of varying degrees of sophistication and accuracy, have been developed to describe deep levels [1–9]. Obtaining a theoretical understanding of deep levels and other defect properties continues to be of interest because of their potential technological importance [11–19].

In earlier work, we outlined a tight-binding-based formalism for calculating the effects of lattice relaxation on deep levels [20–23] and used it to study nearest-neighbor relaxation effects on the deep levels and wavefunctions associated with substitutional impurities. In this paper, we extend this formalism to include second-neighbor relaxation effects. Molecular dynamics is used to calculate the relaxation around specific impurities and the relaxation effects on the deep levels are computed using a tight-binding Green's function technique. Using this theory, deep level chemical trends and trends with varying amounts of lattice relaxation are investigated in Si, GaAs, and GaP. Also, the deep levels produced by several impurities in these materials are calculated and compared with experiment and other theories.

A defect in a semiconductor will interact with the host, displacing the nearby atoms [25]. Since deep levels are produced by the short-ranged part of the defect potential [1–9], they are strongly affected by this distortion. First-principles theories have been used to study these effects [26–28]. Such techniques produce quantitatively reliable results, but they require considerable computational effort. On the other hand, tight-binding approaches are computationally comparatively simple and can easily be used to study trends. The prediction of trends in deep levels was one of the motivations for the present work.

Tight-binding theories have been previously used to study lattice distortions [29] and their effects on deep levels [30–32]. Some of these tight-binding theories can be

* Corresponding author. Tel.: +1-806-742-3767; fax: +1-806-742-1182.

E-mail address: cmyles@gordian.phys.ttu.edu (C.W. Myles).

0022-3697/00/$ - see front matter
PII: S0022-3697(00)00068-8

unsatisfying because of the necessity to treat lattice relaxation phenomenologically. By contrast, our theory retains the computational simplicity of tight-binding methods while calculating lattice relaxation effects using molecular dynamics, thus reducing the phenomenology required to treat these effects.

Our approach is based on our generalization [20–23] of the Hjalmarson et al. [9] deep level theory to include lattice relaxation. We describe the host using the Vogl et al. [33] bandstructure theory. The Hjalmarson et al. theory, which in its original form neglected lattice relaxation, has been widely used and its generalizations have predicted trends in deep levels in many applications [34–56]. In our previous work [20–23] lattice relaxation was incorporated into the Hjalmarson et al. theory by treating the off-diagonal matrix elements of the defect potential with a generalization of Harrison's inverse bond-length-squared scaling rule [57,58]. The relaxed impurity-to-host atom bond length was then computed using molecular dynamics. In this previous work, only the nearest-neighbors of the impurity were allowed to relax.

The present paper extends this work to include the effects of both first- and second-neighbor relaxation. This formalism retains the ability of the Hjalmarson et al. theory to easily predict deep level chemical trends. As in Ref. [9], it does so by computing levels as functions of atomic energy dependent diagonal matrix elements of the defect potential. Trends with varying amounts of lattice relaxation can also be explored by computing levels as functions of interatomic distance-dependent off-diagonal matrix elements of this potential. As in our earlier work, the magnitude of the relaxation for specific impurities is computed using molecular dynamics. This approach retains much of the simplicity of the Hjalmarson et al. theory, while considerably improving its quantitative accuracy.

An earlier extension of the Hjalmarson et al. theory to include lattice relaxation was made by Talwar et al. [30,31], who treated the off-diagonal matrix elements of the defect potential using a generalization of the inverse bond-length-squared scaling rule [57,58] along with a total energy theory [59]. As discussed in Refs. [20–23], the deep levels resulting from this approach fail to improve upon the results of Ref. [9] in comparison with experiment [30–31].

Singh and Madhukar [32] developed a tight-binding-based deep level theory, in which lattice relaxation effects are included, using a transfer-matrix technique. Their calculations are in reasonable agreement with experiment for the As antisite defect in GaAs and for O on the anion site in $GaAs_{1-x}P_x$. Li and Patterson [60,61] have used a formalism similar to that described here to successfully treat deep levels and other defect properties in some of the II–VI semiconductor materials.

2. Formalism

We describe the host with the Vogl et al. [33] sp^3s^*, nearest-neighbor, semi-empirical, tight-binding Hamiltonian H_0. This Hamiltonian has five states per atom (four sp^3 states and an excited s^* state) with 13 parameters, which were obtained by fits to pseudopotential bandstructures [62]. The use of excited s^* states enables a description of the conduction band which is flexible enough to treat both direct and indirect bandgaps. This model reproduces the principal features of the valence and lower conduction bands of several materials.

We consider deep levels produced by neutral, sp^3 bonded, substitutional impurities in zinc-blende and diamond structure hosts. The point group for such impurities is T_d. The deep levels are thus either of the A_1-symmetric (s-like) or the T_2-symmetric (p-like) type. Following previous work, the long-ranged Coulomb potential is neglected, and the deep levels are produced by a short-ranged, central-cell potential [9]. Our formalism could be generalized to include more complicated defects or charge state effects [34–56,60,61].

Our technique is applicable for a general distortion of the host atoms. However, we consider only T_d symmetry-conserving, "breathing-mode" distortions, which are thought to dominate for substitutional impurities [26–28,63–66]. We note that Li and Patterson [60,61] have successfully applied their formalism, which is similar to the present method, to treat lattice relaxation effects on deep levels due to charged impurities, non-ideal vacancies, and interstitial impurities.

2.1. Deep level theory

The Koster–Slater [67] theory is convenient for calculating the energies E produced in the bandgap by a short-ranged defect potential V. In this method, these energies are obtained by solving Schrödinger's equation in the form

$$D(E) = \det[1 - G^0(E)V] = 0, \tag{1}$$

where $G^0(E) = (E - H_0)^{-1}$ is the host Green's function. The advantage of Eq. (1) is that it needs to be solved only in the subspace of the defect potential. In this paper, 17 atoms are allowed to relax: the impurity, four nearest-neighbors, and 12 second-neighbors.

Following previous work [9,20–23,34–56], we include only four orbitals per atom (sp^3 states) in V and neglect the effects of the s^* states on the defect potential. Thus, Eq. (1) is a 68×68 determinant. For breathing-mode distortions, Eq. (1) factors into the product of four 17×17 determinants; one gives the A_1 states and three give the T_2 states (for example see Ref. [24]).

For an impurity on the *anion* site (assumed to be at the origin) in a zinc-blende crystal, the defect potential, including coupling to the first-and second-neighbors, has the form

[24]

$$V = \sum_i (|ia\vec{0}\rangle U_i \langle ia\vec{0}|) + \sum_i \sum_{\vec{d}} (|ia\vec{0}\rangle \alpha_i \langle ic\vec{d}| + \text{H.c.}) + \sum_i \sum_{\vec{d},\vec{d}'} (|ic\vec{d}\rangle \beta_i \langle ia\vec{d}'| + \text{H.c.}), \quad (2)$$

where the sum on i is over the A_1 and T_2 states, a and c refer to anion and cation, $\vec{0}$ is the cell at the origin, the sum on $\vec{d}$ is over the four nearest-neighbors, the sum on $\vec{d}'$ is over the 12 second-neighbors, the U_i are the diagonal matrix elements at the impurity site, the α_i are the matrix elements coupling the impurity with its nearest-neighbor cations, the β_i are the matrix elements coupling these cations with the second-neighbor anions, and H.c. is the Hermitian conjugate. For an impurity on the cation site, the labels a and c are interchanged. We have also done some calculations including matrix elements coupling the impurity directly to its second-neighbors [24]. We have found that these matrix elements are very small in comparison with α_i and β_i, so they are neglected here. The α_i and β_i depend on interatomic distances and are thus measures of the lattice relaxation around the impurity.

The combination of Eqs. (1) and (2) may be viewed as an implicit equation for the deep level E as a function of the parameters U_i, α_i and β_i. That is, Eq. (2) can be used to numerically solve (Eq. (1) to obtain $E = E(U_i, \alpha_i, \beta_i)$. By doing this, the chemical trends in the deep levels (variation with U_i) and their trends with varying amounts of relaxation (variation with α_i and β_i) can be explored.

In order to calculate the deep levels produced by a particular impurity, U_i, α_i, and β_i must be specified. We use the empirical rule [9] that the U_i are proportional to the atomic-energy difference between the impurity and the replaced host atom. That is

$$U_i = \gamma_i(\epsilon_{\mathrm{I}}^i - \epsilon_{\mathrm{H}}^i), \quad (3)$$

where ϵ_{I}^i and ϵ_{H}^i are the i-symmetric atomic energies [57,58] for the impurity and the host atoms and γ_i is a constant. In Ref. [9], it is shown that $\gamma_{A_1} = 0.8$ and $\gamma_{T_2} = 0.6$. The use of Eq. (3) along with the numerical solutions for $E(U_i, \alpha_i, \beta_i)$ gives the chemical trends. To model α_i and β_i, we use a generalization of Harrison's inverse-bond-length-squared scaling rule [57,58], which gives [24]

$$\alpha_i = -C_i[(d_{\mathrm{I}})^{-2} - (d_{\mathrm{H}})^{-2}] \quad (4)$$

and

$$\beta_i = -C_i[(d_{\mathrm{II}})^{-2} - (d_{\mathrm{H}})^{-2}], \quad (5)$$

where d_{I} is the impurity atom-to-host atom bond length, d_{II} is the first- to second-neighbor bond length, d_{H} is the host bond length, and C_i is a material independent constant. We find [24] that, for the bandstructures of Ref. [33], $C_{A_1} = 10.5\ \mathrm{eV(\AA)^2}$ and $C_{T_2} = -3.0\ \mathrm{eV(\AA)^2}$. The use of Eqs. (4) and (5) along with $E(U_i, \alpha_i, \beta_i)$ will give the lattice relaxation trends.

Clearly, α_i and β_i are measures of the effects of first- and second-neighbor relaxation. From Eqs. (4) and (5) and the signs of the C_i, it can be seen that for outward first-neighbor relaxation ($d_{\mathrm{I}} \geq d_{\mathrm{H}}$), $\alpha_{A_1}(\alpha_{T_2})$ is positive (negative), while for inward relaxation ($d_{\mathrm{I}} \leq d_{\mathrm{H}}$) $\alpha_{A_1}(\alpha_{T_2})$ is negative (positive). Similar statements also hold regarding β_i with second-neighbor outward or inward relaxation. To calculate α_i and β_i for specific impurities, we use experimental values [57,58] for d_{H} and compute d_{I} and d_{II} by the molecular dynamics scheme we now describe.

2.2. Forces on atoms: molecular dynamics

For an ideal substitutional impurity, all host atoms remain in their perfect-crystal positions. When the deep level problem is treated more realistically, if one starts with the nearby atoms in their equilibrium positions, they will experience a net force, which will cause the lattice to relax to a new configuration where that force is zero. In Refs. [20–23], only the nearest-neighbor lattice relaxation was considered and the force acting on each of the four nearest-neighbor host atoms was assumed, for "breathing mode" distortions, to be along the impurity to first-neighbor bond.

In the present case, where both first- and second-neighbor relaxation are included, the net force acting on a nearest-neighbor atom is more complicated. For breathing mode distortions, this force is the vector sum of four forces; one acting along the impurity to first-neighbor bond and three acting along the three bonds from the first- to the second-neighbors. The bond angles also change during relaxation, so the vector sum must be done carefully at each time step of the relaxation. On the other hand, the total force acting on each of the 12 second-neighbors is, in this approximation, directed along a first- to second-neighbor bond. These forces can thus be treated in a manner analogous to our treatment of first-neighbor forces in Refs. [20–23]. More details of how we account for the vector nature of the forces may be found in Ref. [24].

The total force on any one of the first- or second-neighbors can be divided into repulsive and attractive parts. Thus, for example, the component along the x direction can be written

$$F_x = F_x^{\mathrm{r}} + F_x^{\mathrm{a}}. \quad (6)$$

The origin of the repulsive force, F_x^{r}, is the repulsion between electrons in overlapping states. We compute it from a pair potential based on Harrison's overlap interaction [57,58], which gives

$$F_x^{\mathrm{r}} = -A/d^5, \quad (7)$$

where d is either d_{I} or d_{II}, depending on whether a first- or second-neighbor is being considered, and A is a constant determined by requiring the total force to vanish when the impurity is replaced by a host atom ($d_{\mathrm{I}} = d_{\mathrm{II}} = d_{\mathrm{H}}$). We find

Table 1
Deep energy levels of A_1 symmetry, bond lengths, and bond length changes for various impurities in Si, GaAs and GaP. All energies are in electron volts, measured from the top of the valence band. The bond lengths are in Å. $\Delta d = d_I - d_H$, $\Delta d' = d_{II} - d_H$

System	Present theory	Experiment	Hjalmarson [9]	d_I	Δd	d_{II}	$\Delta d'$
Si:S	0.64	0.85[a]	0.58	2.23	−0.12	2.41	0.06
Si:Se	0.84	0.86[a]	0.65	2.03	−0.32	2.48	0.13
Si:Te	1.04	1.01[a]	1.12	2.60	0.25	2.28	−0.09
GaAs:O	1.16	0.75[b]	1.26	2.73	0.28	2.36	−0.11
GaAs:As_{Ga}	0.74	0.75[b]	0.79	2.39	−0.06	2.47	0.02
GaP:N	2.25	2.34[c]	2.10	2.15	−0.21	2.41	0.05
GaP:O	1.70	1.46[c]	1.85	2.78	0.42	2.23	−0.13
GaP:P_{Ga}	1.09	1.10[d]	1.03	2.28	−0.08	2.40	0.04
GaP:Ge	1.95	2.16[e]	1.85	2.24	−0.12	2.45	0.06

[a] Ref. [1].
[b] Ref. [78].
[c] Ref. [79].
[d] Quoted in Refs. [80,81].
[e] Ref. [82].

that $A = 199.0$, 146.0 and 152.0 eV(Å)^4 for Si, GaAs, and GaP, respectively.

We compute the attractive force, F_x^a, which originates from the occupied one electron levels, directly from the electronic structure *in the presence of the impurity* by using the Hellmann–Feynman theorem [68–72]. For example, the x component of this force is computed from the derivative of the total quantum-mechanical energy, E_{tot}, as

$$F_x^a = -\frac{\partial E_{tot}}{\partial x} = -\frac{\partial}{\partial x}\int_{-\infty}^{E_F} E\rho(E)\,dE, \tag{8}$$

where E_F is the Fermi energy and $\rho(E) = -(1/\pi)$ Im Tr $G(E)$ is the density of states. Here, $G(E)$ is the Green's function, *in the presence of the impurity*, which can be found from Dyson's equation

$$G(E) = G^0(E) + G^0(E)VG(E) = [1 - G^0(E)V]^{-1}G^0(E). \tag{9}$$

By combining Eq. (8) with Eq. (9) and its x derivative, and by using the invariance of the trace and performing a partial integration, F_x^a can be written as

$$F_x^a = -\frac{1}{\pi}\,\text{Im Tr}\int_{-\infty}^{E_F} G\frac{\partial V}{\partial x}\,dE. \tag{10}$$

(10)

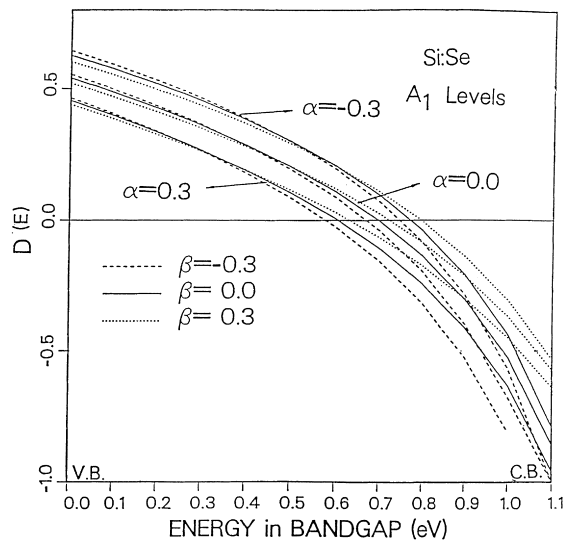

Fig. 1. $D(E)$ as a function of energy E in the bandgap for A_1-symmetric levels due to Si:Se ($U = -6.5$ eV). The different curves indicate the values of matrix elements α and β. The deep level in each case occurs when $D(E) = 0.0$.

Using this formalism and beginning with the first- and second-neighbor host atoms in their perfect crystal positions, one can calculate the motion of these atoms for a small time interval, Δt, using Newton's Second Law along with standard molecular dynamics methods [73–77]. In this manner, new atomic positions, new bond lengths d_I and d_{II}, a new defect potential V, and new forces can be computed. This process can be repeated for successive intervals Δt until the net force acting on each atom approaches zero. In this manner, one can determine d_I, d_{II} and V for the relaxed lattice. Then, the deep levels can be obtained from Eqs. (1)–(5).

3. Results for trends

We have used the formalism just described to investigate the effects of first- and second-neighbor relaxation on the deep levels produced by substitutional impurities in Si, GaAs, GaP, AlP, AlAs, GaSb, and InP. Here, we present our results for Si, GaAs, and GaP. The results for the other materials are qualitatively similar to those presented here [24]. Interested readers are referred to Ref. [24] for these

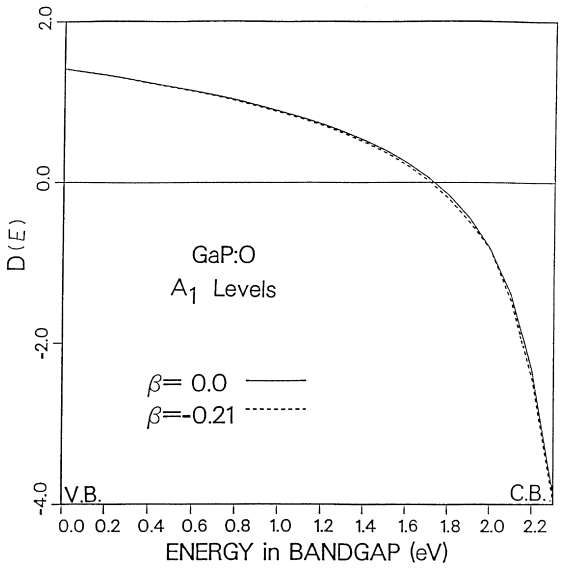

Fig. 2. $D(E)$ as a function of energy E in the bandgap for GaP:O for $\beta = -0.21$ and 0.0 eV ($U = -11.9$ eV and $\alpha = 0.53$ eV). The deep level in the two cases occurs when $D(E) = 0.0$.

results. We have found [24] that lattice relaxation effects for impurities in III–V compounds and Group IV materials are much more important for A_1 levels than for T_2 levels. Thus, only results for A_1 levels are discussed here. In what follows, U_{A_1}, α_{A_1}, and β_{A_1} are denoted as U, α, and β and the zero of energy E is taken as the top of the valence band. Our molecular dynamics results for the deep levels and equilibrium bond lengths for several impurities in Si, GaAs, and GaP are summarized in Table 1 and are discussed in detail below.

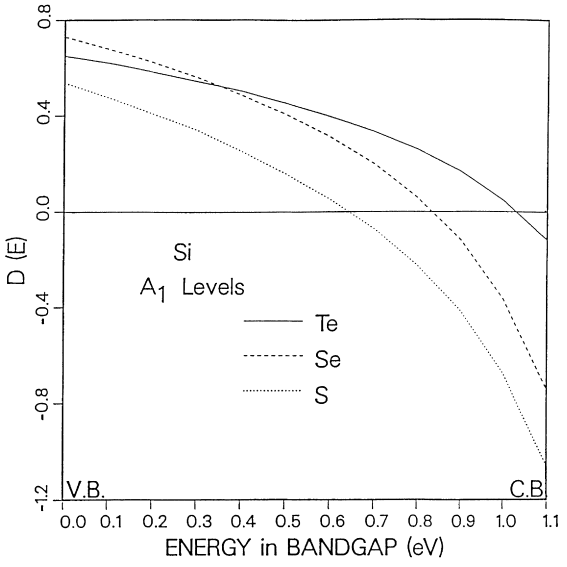

Fig. 3. $D(E)$ as a function of energy E in the bandgap for Si:Se, Si:S, and Si:Te. The deep level in each case occurs when $D(E) = 0.0$.

3.1. Trends with first- and second-neighbor relaxation

Typical results, illustrating trends in the deep levels with varying amounts of relaxation, are shown in Fig. 1, in which $D(E)$ (Eq. (1)) is plotted versus E in the bandgap for various values of α and β for the A_1-symmetric level produced by Se in Si. In this case, Eq. (3) gives $U = -6.5$ eV. There are three groups of curves containing three members each. Each group corresponds to a different value of the first-neighbor matrix element α. From left to right, the groups represent $\alpha = 0.3$, 0.0, and -0.3 eV, respectively, corresponding to $d_I/d_H = 1.09$, 1.00 and 0.93. Within each group, the curves correspond to different values of the second-nearest neighbor matrix element β. These are $\beta = -0.3$ (dashed curve), 0.0 (solid curve), and 0.3 eV (dotted curve), corresponding to $d_{II}/d_H = 0.93$, 1.00, and 1.09, respectively. The intersections of these curves with $D(E) = 0.0$ give the deep levels in the bandgap for these values of α and β. It can be seen that, as α becomes more negative (larger inward first-neighbor relaxation), the deep level moves towards the conduction band, while as it becomes more positive (larger outward nearest-neighbor relaxation), it moves towards the valence band. Thus, these results show that inward nearest-neighbor relaxation ($d_H \geq d_I$) about an impurity moves the A_1 deep level towards the conduction band, while outward relaxation ($d_H \leq d_I$) moves it towards the valance band, in agreement with previous results [20–23].

The opposite trend as a function of β can also be seen in Fig. 1; the deep level moves towards the conduction band as β becomes more positive (larger outward second-neighbor relaxation, $d_H \leq d_{II}$)) and towards the valence band as β becomes more negative (larger inward relaxation $d_H \geq d_{II}$). Clearly, from Fig. 1, the effects of second-neighbor relaxation on the deep level are much smaller than first-neighbor effects, even if the first- and second-neighbor matrix elements are of similar magnitude. We have found that this result and the trends shown in Fig. 1 hold qualitatively for all impurities and hosts we have considered.

To further illustrate the small effect of second-neighbor relaxation on deep levels, consider the A_1-symmetric level produced by O substitutional for P in GaP. In this case, Eq. (3) gives $U = -11.9$ eV. From Table 1, the molecular dynamics results yield $d_I = 2.78$ Å and $d_{II} = 2.23$ Å. Since $d_H = 2.36$ Å, this corresponds to a very large outward first-neighbor relaxation of about 17% and to a large inward second-neighbor relaxation of 5%. These are (by far!) the largest percentage relaxations of any case we have studied. As was discussed in Refs. [20–24], GaP:O is anomalous in several ways, so this large relaxation is not surprising. Using these results in Eqs. (4) and (5) gives $\alpha = 0.53$ eV and $\beta = -0.21$ eV. This yields a deep level at 1.70 eV (see Table 1), still far removed from the experimental value of 1.46 eV [80,81], but closer to that value than the 1.85 eV predicted by the Hjalmarson et al. [9] theory.

Fig. 2 shows the results for $D(E)$ versus E for GaP:O. The results for both $\beta = -0.21$ (dashed curve) and $\beta = 0.0$ eV

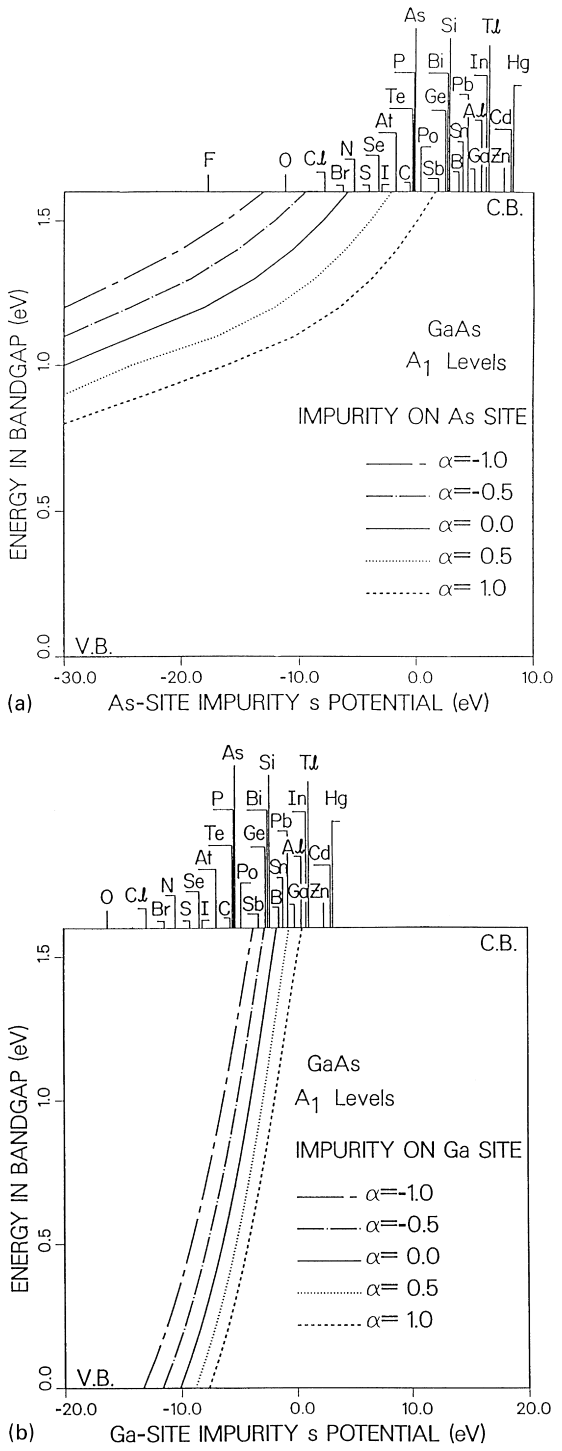

Fig. 4. Deep levels versus U for A_1-symmetric states in GaAs for $\beta = 0.0$ and for $\alpha = 1.0$ (dashed curves), 0.5 (dotted curves), 0.0 (solid curves), -0.5 (chained curves), and -1.0 eV (long dashed-short dashed curves). These correspond to $d_I/d_H = 1.53$, 1.20, 1.00, 0.90, and 0.81. (a) As-site impurities. (b) Ga-site impurities.

(solid curve) are shown. Using the latter β value corresponds to neglect of second-neighbor relaxation. The deep levels are again determined by the intersection of these curves with $D(E) = 0.0$. From the figure, it is clear that the inclusion of the second-neighbor relaxation shifts the deep level by a very small amount. Numerically, one obtains 1.71 eV for $\beta = 0.0$ eV (no second-neighbor relaxation) and 1.70 eV (Table 1) for $\beta = -0.21$ eV. Thus, even though the second-neighbors of O have relaxed considerably and the resulting second-neighbor matrix element β is not small, the shift that this induces in the deep level is still very small. We have found this to be true for all the impurities and hosts we have considered.

An example of the chemical trends obtained using this theory is displayed in Fig. 3, which shows our results for $D(E)$ versus E for the A_1-symmetric levels produced by Si:Te (solid curve), Si:Se (dashed curve), and Si:S (dotted curve). The values of U from Eq. (3) are -3.5 eV (Si:Te), -6.5 eV (Si:Se), and -7.4 eV (Si:S). The molecular dynamics results are (Table 1) $d_I = 2.60$, 2.03, and 2.23 Å and $d_{II} = 2.28$ eV, 2.48 eV, and 2.41 Å for Si:Te, Si:Se, and Si:S, respectively. Using these results in Eqs. (4) and (5) gives $\alpha = 0.35$ eV, -0.65 eV, and -0.21 eV and $\beta = -0.12$ eV, 0.19 eV, and 0.09 eV for the same cases. In Fig. 3, the deep levels are again found where $D(E) = 0.0$. This figure predicts that, as the relative electronegativity between the impurity and the replaced host atom increases, the level moves deeper into the bandgap. That is, as the atomic energy difference between the impurity and the host atom increases (as U becomes increasingly negative), the level moves away from the conduction band edge. From Fig. 3, the predicted level ordering, from shallowest to deepest, is Si:Te, Si:Se, and Si:S in order of increasing $|U|$. This is in qualitative agreement with the original predictions of Hjalmarson et al. [9].

We have found qualitatively similar chemical and first- and second-neighbor lattice relaxation trends for all the cases that we have considered. Thus, we conclude that lattice relaxation effects do not alter the qualitative, "defect molecule" picture of deep levels, developed by Hjalmarson et al. [9] and others [1]. In this picture, electronegativity differences are the primary mechanisms responsible for the ordering of deep levels. Numerically, from Fig. 3, one obtains (Table 1) deep levels at 0.65 eV, 0.84 eV, and 1.04 eV for Si:S, Si:Se, and Si:Te, respectively. These are in very good agreement with the data quoted in Ref. [1].

3.2. Chemical trends: trends with varying amounts of lattice relaxation

Fig. 4 shows results for the A_1-symmetric levels produced by substitutional impurities in GaAs. The results for impurities on the anion and cation sites are shown in Fig. 4a and b, respectively. In both part figures, the deep level (E) dependence on U is shown for various values of the first-neighbor matrix element α. Since, as was just illustrated, the

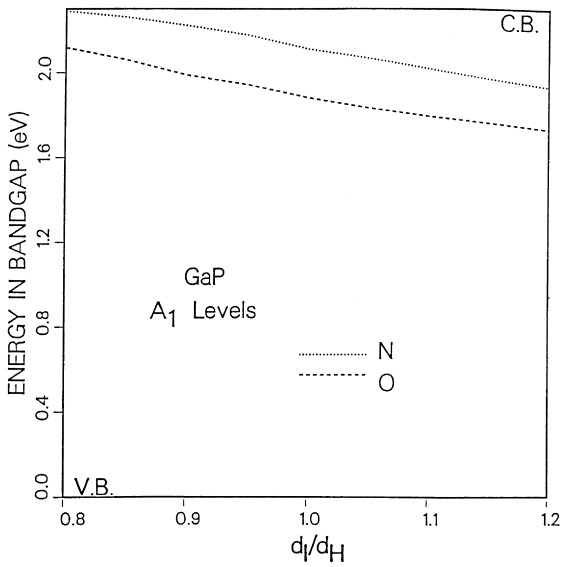

Fig. 5. Deep levels of A_1 symmetry produced by N (dotted curve) and O (dashed curve) substitutional for P in GaP. The abscissa is d_I/d_H and the ordinate is the bandgap energy. The quantity β has been set to zero.

second-neighbor matrix element β has only a small effect on the deep levels, it has been set to zero in Fig. 4a and b. In this figure, the $\alpha = 1.0$ eV, 0.5 eV, 0.0 eV, -0.5 eV, and -1.0 eV results are shown, respectively, as dashed, dotted, solid, dotted-dashed, and chained curves. These correspond to bond length ratios of $d_I/d_H = 1.53$, 1.20, 1.00, 0.90, and 0.81, respectively. The vertical scale is the deep level energy in the bandgap. The horizontal scale and the labeled impurities at the top of the figures correspond to the value of U calculated from atomic energy differences [9] (Eq. (3)). Similar results for Si and GaP were discussed in Ref. [20–23]. The results for the A_1-symmetric levels in AlP, AlAs, GaSb, and InP are qualitatively similar to those presented here [24].

The deep levels for a particular impurity for a particular α value can be obtained from Fig. 4a and b by finding the intersection with the curve for that α of a vertical line drawn from the label for that impurity at the top of the figure. If there is no intersection, no A_1 level is predicted in the bandgap for that α.

Inspection of Fig. 4a and b reveals the qualitative effects of nearest-neighbor lattice relaxation on A_1 levels. Chemical trends (variation in E for fixed α as U varies) and trends for varying amounts of relaxation (variation in E for fixed U as α varies) can both be extracted from these figures. For example, the $\alpha \neq 0$ curves have similar chemical trends as those of the $\alpha = 0$ (no relaxation) curve (which is the same as the results of Ref. [9]). Also, the deep levels, for fixed U, are shifted upward in the bandgap as α becomes increasingly negative (increasing magnitude of inward relaxation, $d_H \geq d_I$) and downward as α becomes more

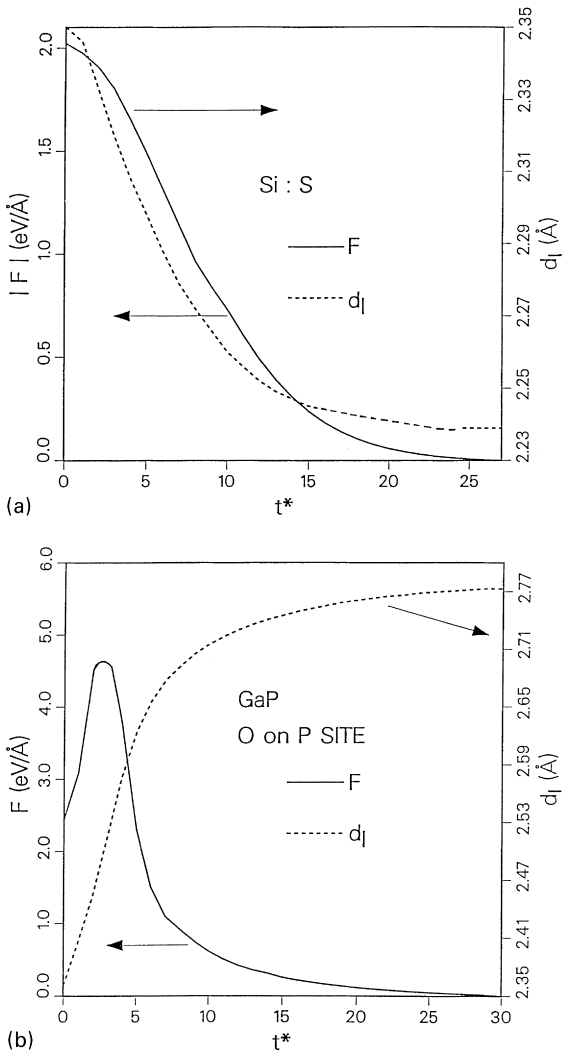

Fig. 6. Time dependence of the magnitude of the total force (solid curves) along an impurity atom–host atom bond and of the bond length (dashed curves) for: (a) substitutional S in Si; and (b) O substitutional for P in GaP.

positive (increasing magnitude of outward relaxation $d_H \leq d_I$), in agreement with the trend discussed above.

This trend can be illustrated by discussing a few cases in detail. For example, consider the O impurity substitutional for As in GaAs. From Fig. 4a, this impurity is predicted to have a deep level which changes considerably as α is changed and which moves towards the conduction band for increasing inward relaxation. It is predicted to change from about 1.1 eV for $\alpha = 1.0$ eV (outward relaxation; $d_I = 1.53 d_H$), to about 1.4 eV for $\alpha = 0.0$ (no relaxation; $d_I = d_H$), to just above the conduction band edge for $\alpha = -1.0$ eV (inward relaxation; $d_I = 0.81 d_H$). Our molecular dynamics results (Table 1) predict the O deep level at

1.16 eV, which is closer to the experimental value [78] than that predicted by the Hjalmarson et al. [9] theory.

Similar trends can be obtained for Ga-site impurities in GaAs by examination of Fig. 4b. For example, consider the As on Ga antisite defect "impurity". It can be seen that a large variation in the associated deep level is predicted, depending on the amount of relaxation. The deep level changes from about 0.25 eV for $\alpha = 1.0$ eV (outward relaxation; $d_I = 1.53 d_H$), to about 0.75 eV for $\alpha = 0.0$ eV (no relaxation; $d_I = d_H$), to about 1.25 eV for $\alpha = -1.0$ eV (inward relaxation; $d_I = 0.81 d_H$). Our molecular dynamics results (Table 1) predict this level at 0.74 eV, in fortuitously good agreement with the experimental value of 0.75 eV [78].

The type of trends just discussed are also illustrated in a different way in Fig. 5, which shows results for the A_1 levels produced by N and O on the P site in GaP. In this case, the second-neighbor matrix element β has also been set to zero. In this figure, the ordinate is the energy in the bandgap and the abscissa is d_I/d_H. The curves show the dependence of the deep levels on this ratio. As can be seen, this dependence is nearly linear. Further, these levels move towards the conduction band for inward relaxation and towards the valence band for outward relaxation, in agreement with the above discussion.

4. Molecular dynamics results

4.1. Time dependence of force and bond length

As a typical illustration of the molecular dynamics results, in Fig. 6 we show the time dependence of the magnitude of the total force along an impurity atom-to-host atom bond (solid curves) and of d_I (dashed curves) for Si:S (Fig. 6a) and GaP:O (O substitutional for P) (Fig. 6b). These are plotted versus $t* = t/(\Delta t)$, where $\Delta t = 0.35 \times 10^{-14}$ s is the time step we have used in the molecular dynamics calculations. This value of Δt was obtained by trial and error. We have found that, while the best choice depends on the particular case, Δt is always of this order of magnitude. A smaller Δt uses considerably more computer time to achieve similar results and a larger value can cause an "overshoot" of the final equilibrium position and an oscillatory behavior of d_I versus t^*.

Fig. 6 reveals the details of the dynamics of the lattice relaxation, and shows several interesting features. In both Fig. 6a and b, after only 25 time steps or ~0.09 ps, the force approaches zero. Also, as the nearest-neighbor host atoms approach their new equilibrium positions, they move a considerable distance. For Si:S, they move inward by about 0.12 Å, or ~5% of the 2.35 Å Si–Si bond length. For GaP:O, they move outward by about 0.42 Å, or ~17% of the 2.36 Å Ga–P bond length. The results for Si:S are in qualitative agreement with a covalent radius model [20–23]. The large relaxation for GaP:O is consistent with the anomalous behavior of O in this material [20–23,63,64].

It is interesting that, as a function of time, the magnitude of the force in GaP:O (Fig. 6b) first increases to a maximum and then decreases to zero, rather than smoothly decreasing to zero as for Si:S (Fig. 6a). This can be understood by noting that lattice relaxation is a competition between attractive and repulsive forces. In the final results of this competition, the net force approaches zero and the atoms approach new equilibrium positions. However, during this process, the net force at any time step may be either larger or smaller than that at the previous time step.

We note that self-consistent Green's function approaches [26–28] obtain the same order of magnitude for the forces and similar trends for forces versus time, as we illustrate in Fig. 6.

4.2. Comparison with experiment and other theories

Results obtained using our formalism to compute A_1 levels produced by several impurities in Si, GaAs, and GaP are shown in Table 1. Also shown are the experimental deep levels [78–82] and the predictions of the Hjalmarson et al. [9] theory. The last four columns give our results for d_I, $\Delta d = d_I - d_H, d_{II}$, and $\Delta d' = d_{II} - d_H$. An inward nearest-neighbor relaxation is clearly predicted for all the cases considered, except for Si:Te, GaAs:O, and GaP:O. Except for the latter two cases, all of the results for d_I shown in Table 1 are in qualitative agreement with a covalent radius model [20–23]. Where comparisons are possible, our results for d_I are in reasonable agreement with those of Refs. [30,31].

In all cases considered in Table 1, our deep level predictions considerably improve upon those of Ref. [9] in comparison with experiment. In some cases, there is very good quantitative agreement with the data. The remaining discrepancies between theory and experiment might be due to inaccuracies in the host bandstructures and/or to charge state effects.

Self-consistent pseudopotential Green's function methods [26–28] have been used to accurately predict deep levels and relaxation distances for some impurities in some materials. Where comparisons are possible, our results compare quite favorably, qualitatively and quantitatively, with results from this more sophisticated theory. For example, Scheffler et al. [26–28] have used this method to study the effects of lattice relaxation on the deep level produced by Ge on the Ga site in GaP. They predict that the nearest-neighbor P atoms relax towards the Ge_{Ga} center, and that an A_1 level is produced at 2.26 eV above the valence band, in reasonable agreement with the experimental value of 2.16 eV [82]. They also predict an impurity bond length of $d_I = 2.28$ Å, which is reduced from the GaP bond length (2.36 Å) by about 3.5%.

As can be seen in Table 1, our results are in reasonable agreement with all of these predictions. Our predicted deep level for GaP:Ge is 1.95 eV, also in reasonable agreement

with experiment [82], and our predicted bond length is $d_I = 2.24\,\mathring{A}$, a 5% reduction in comparison with the host bond length. The order of magnitude of the initial forces due to substitutional impurities, and the trends of the force versus relaxation distance obtained by our theory are also in agreement with those obtained by self-consistent pseudopotential Green's function methods [65,66].

5. Summary and conclusions

We have investigated the effects of lattice relaxation on the A_1-symmetric deep levels in several semiconductors using an extension of a previously developed formalism. Our method is a generalization of the Hjalmarson et al. [9] theory. For simplicity, only symmetry-conserving breathing mode relaxations have been considered, although our method could be generalized to treat more complicated cases. Both first- and second-neighbor lattice-relaxation are included by representing the off-diagonal matrix elements of the defect potential by parameters α and β, which depend on the host and host-impurity bond lengths. To determine these as functions of the bond lengths, we have used Harrison's inverse-bond-length squared-scaling rule [57,58]. By computing deep levels as functions of α and β, the effects of varying amounts of lattice relaxation have been explored. We find that second-neighbor relaxation affects the deep levels by only a small amount in comparison to first-neighbor effects.

Molecular dynamics has been used to calculate the first- and second-neighbor relaxation around particular impurities. That is, this method has been used to determine the relaxed bond lengths which enter the off-diagonal quantities α and β. The attractive part of the force is computed directly from the electronic structure, using the Hellmann–Feynman theorem [68–72]. The repulsive part is obtained from a pair potential based on Harrison's overlap interaction [57,58].

Since the Hjalmarson et al. [9] theory and its generalizations have been successful both in predicting the chemical trends of deep levels and in making semiquantitative predictions for such levels [9,34–56], we believe that our predicted trends should be reliable. Further, our numerical calculations of deep levels including such effects are in reasonable agreement with experiment and considerably improve the quantitative accuracy of the Hjalmarson et al. theory. Some of these predictions are also in reasonable agreement with those obtained from first-principles theories. We hope that these predictions will be useful in assisting in the identification of deep levels.

We note that our results depend on a generalization of the inverse-bond-length squared scaling rule [57,58] for α and β (Eqs. (4) and (5)) and on our assumption of a repulsive force obtained from Harrison's overlap interaction [57,58] (Eq. (7)). However, our general formalism could also be utilized with other reasonable assumptions for these quantities. To test the sensitivity of our results to these assumptions, we have repeated some of our calculations assuming exponential dependencies [83] of these quantities on d_I and d_{II}. The results obtained in this manner for these bond lengths and for the corresponding deep levels differ by less than 1% from those in Table 1.

Acknowledgements

We thank the Ballistic Missile Defense Organization for a grant (Grant no. N00014-93-1-0518) through the Office of Naval Research and the State of Texas Advanced Research Program for a grant (Grant no. 003644-047), both of which partially supported this work.

References

[1] M. Jaros, Deep Levels in Semiconductors, Hilger, Bristol, 1980.
[2] S.T. Pantelides, Deep Centers in Semiconductors, Gordon and Breach, New York, 1986.
[3] S.T. Pantelides, Rev. Mod. Phys. 50 (1978) 797.
[4] D.J. Chadi, in: J.R. Chelikowski, S.G. Louie (Eds.), Quantum Theory of Real Materials, Kluwer, Norwell, MA, 1996.
[5] L.A. Hemstreet, Phys. Rev. B 15 (1977) 834.
[6] G.A. Baraff, M. Schlüter, Phys. Rev. Lett. 41 (1978) 892.
[7] G.A. Baraff, M. Schlüter, Phys. Rev. B 30 (1984) 1853.
[8] J. Bernholc, N.O. Lipari, S.T. Pantelides, Phys. Rev. Lett. 41 (1978) 895.
[9] H.P. Hjalmarson, P. Vogl, D.J. Wolford, J.D. Dow, Phys. Rev. Lett. 44 (1980) 810.
[10] W. Kohn, in: F. Seitz, D. Turnbull (Eds.), Solid State Physics, Academic, New York, 1957 (vol. 5, chap. 4).
[11] J.C. Bourgoin, M. Zazoui, J. Phys. III (France) 7 (1997) 2145.
[12] Y. Shinozuka, T. Karastu, Mater. Sci. Forum 258–263 (1997) 659.
[13] M. Saito, Phys. Rev. B 56 (1997) 13073.
[14] V. Gubanov, E.A. Panatori, C.Y. Fong, B.M. Klein, Phys. Rev. B 56 (1997) 13077.
[15] A. Fazzio, P. Piquini, R. Mota, Phys. Rev. B 56 (1997) 13073.
[16] D. Sasireka, M. Thiagarajan, E. Palaniyandi, K. Iyakutti, Phys. Status Solidi (b) (Germany) 210 (1998) 111.
[17] D.D. Nolte, Phys. Rev. B 58 (1998) 7994.
[18] A. Lichanot, R. Orlando, R. Dovesi, J. Phys. Chem. Solids 59 (1998) 7.
[19] J. Neugebauer, C. Van de Walle, J. Appl. Phys. 85 (1999) 3003.
[20] W.-G. Li, C.W. Myles, Phys. Rev. B 43 (1991) 2192.
[21] W.-G. Li, C.W. Myles, Phys. Rev. B 43 (1991) 9947.
[22] W.-G. Li, C.W. Myles, Mater. Sci. Forum (1992) 83–87.
[23] W.-G. Li, C.W. Myles, Phys. Rev. B 47 (1993) 4281.
[24] W.-G. Li, PhD dissertation, Texas Tech University, 1991.
[25] F.P. Larkins, A.M. Stoneham, J. Phys. C 4 (1971) 143.
[26] M. Scheffler, J.P. Vigneron, G.B. Bachelet, Phys. Rev. B 31 (1985) 6541.
[27] U. Lindfelt, Phys. Rev. B 28 (1982) 4570.
[28] U. Lindfelt, Phys. Rev. B 30 (1984) 1102.

[29] E.A. Kraut, W.A. Harrison, J. Vac. Sci. Technol. B 3 (1985) 1267.
[30] D.N. Talwar, K.S. Suh, C.S. Tang, Phil. Mag. B 54 (1986) 93.
[31] D.N. Talwar, K.S. Suh, C.S. Tang, Phil. Mag. B 56 (1987) 593.
[32] J. Singh, A. Madhukar, Phys. Rev. B 25 (1982) 7700.
[33] P. Vogl, H.P. Hjalmarson, J.D. Dow, J. Phys. Chem. Solids 44 (1983) 365.
[34] O.F. Sankey, J.D. Dow, Appl. Phys. Lett. 38 (1981) 685.
[35] O.F. Sankey, J.D. Dow, J. Appl. Phys. 52 (1981) 5139.
[36] O.F. Sankey, J.D. Dow, Phys. Rev. B 26 (1982) 3243.
[37] O.F. Sankey, J.D. Dow, Phys. Rev. B 27 (1983) 7641.
[38] C.W. Myles, O.F. Sankey, Phys. Rev. B 29 (1984) 6810.
[39] C.W. Myles, P.F. Williams, E.G. Bylander, R.A. Chapman, J. Appl. Phys. 57 (1985) 5279.
[40] Y.-T. Shen, C.W. Myles, Appl. Phys. Lett. 51 (1987) 2304.
[41] Y.-T. Shen, C.W. Myles, J. Appl. Phys. 65 (1989) 4273.
[42] Y.-T. Shen, C.W. Myles, Phys. Rev. B 40 (1989) 6222.
[43] Y.-T. Shen, C.W. Myles, Phys. Rev. B 40 (1989) 10425.
[44] E.G. Bylander, C.W. Myles, Y.-T. Shen, J. Appl. Phys. 67 (1990) 7351.
[45] W.C. Ford, C.W. Myles, Phys. Rev. B 34 (1986) 927.
[46] W.C. Ford, C.W. Myles, Phys. Rev. B 38 (1988) 1210.
[47] W.C. Ford, C.W. Myles, Phys. Rev. B 38 (1988) 10533.
[48] W.C. Ford, C.W. Myles, Phys. Rev. B 40 (1989) 11947.
[49] R.E. Allen, T.J. Humphreys, J.D. Dow, O.F. Sankey, J. Vac. Sci. Technol. B 2 (1984) 449.
[50] O.F. Sankey, R.E. Allen, J.D. Dow, J. Vac. Sci. Technol. B 2 (1984) 491.
[51] C.W. Myles, S.-F. Ren, R.E. Allen, S.-Y. Ren, Phys. Rev. B 35 (1987) 9758.
[52] P.G. Snyder, C.W. Myles, M.A. Gundersen, H.-H. Dai, Phys. Rev. B 32 (1985) 2685.
[53] H.-H. Dai, M.A. Gundersen, C.W. Myles, Phys. Rev. B 33 (1986) 823.
[54] H.-H. Dai, M.A. Gundersen, C.W. Myles, Phys. Rev. B 47 (1988) 1205.
[55] S. Lee, J.D. Dow, O.F. Sankey, Phys. Rev. B 31 (1985) 3910.
[56] C.W. Myles, J. Vac. Sci. Technol A 6 (1988) 2675.
[57] W. Harrison, Electronic Structure and the Properties of Solids, Freeman, San Francisco, CA, 1980.
[58] W. Harrison, Electronic Structure and the Properties of Solids, Phys. Rev. B 27 (1983) 3592.
[59] J.M. Baranowski, J. Phys. C 17 (1984) 6281.
[60] W.-G. Li, J.D. Patterson, Phys. Rev. B 50 (1995) 14903.
[61] W.-G. Li, J.D. Patterson, Phys. Rev. B 53 (1996) 15622.
[62] J.R. Chelikowski, M.L. Cohen, Phys. Rev. B 14 (1976) 556.
[63] T.N. Morgan, Phys. Rev. Lett. 49 (1982) 173.
[64] T.N. Morgan, Phys. Rev. B 29 (1984) 5667.
[65] G.A. Baraff, E.O. Kane, M. Schluter, Phys. Rev. Lett. 47 (1981) 801.
[66] G.A. Baraff, E.O. Kane, M. Schluter, Phys. Rev. B 25 (1982) 548.
[67] G.F. Koster, J.C. Slater, Phys. Rev. 95 (1957) 1167.
[68] H. Hellmann, Einfuhrung in Die Quantenchemie, (Franz Deutsche, 1937).
[69] R.P. Feynman, Phys. Rev. 56 (1939) 340.
[70] J.I. Musher, J. Chem. Phys. 43 (1965) 2145.
[71] J.I. Musher, Am. J. Phys. 34 (1966) 267.
[72] B.M. Deb, Rev. Mod. Phys. 45 (1973) 22.
[73] D.C. Rapaport, The Art of Molecular Dynamics Simulation, Cambridge University Press, Cambridge, UK, 1995.
[74] D.W. Heermann, Computer Simulation Methods in Theoretical Physics, 2nd ed., Springer, New York, 1990.
[75] J.M. Haile, Molecular Dynamics Simulation, Wiley, New York, 1992.
[76] Y.K. Park, C.W. Myles, Phys. Rev. B 51 (1995) 1671.
[77] Y.K. Park, C.W. Myles, Phys. Rev. B 48 (1993) 1247.
[78] E. Weber, H. Ennen, U. Kaufmann, J. Appl. Phys. 53 (1982) 6142.
[79] A.G. Milnes, Deep Impurities in Semiconductors, Wiley, New York, 1973.
[80] M. Scheffler, J.P. Vigneron, G.B. Bachelet, Phys. Rev. Lett. 49 (1982) 1765.
[81] M. Scheffler, J. Bernholc, N.O. Lipari, S.T. Pantelides, Phys. Rev. B 29 (1984) 3269.
[82] G.F. Neumark, V.K. Kosai, Semiconductors and Semimetals, Academic Press, New York, 1983 (vol. 19).
[83] M. Menon, R.E. Allen, Phys. Rev. B 33 (1986) 5611.